Quantification of Structural Loading During Off-Road Cycling

D. S. De Lorenzo
Research Assistant.

M. L. Hull
Professor of Mechanical Engineering and Chair of Biomedical Engineering.

Department of Mechanical Engineering, University of California, Davis, Davis, CA 95616

To provide data for fatigue life prediction and testing of structural components in off-road bicycles, the objective of the research described herein was to quantify the loads input to an off-road bicycle as a result of surface-induced loads. A fully instrumented test bicycle was equipped with dynamometers at the pedals, handlebars, and hubs to measure all in-plane structural loads acting through points of contact between the bicycle and both the rider and the ground. A portable data acquisition system carried by the standing rider allowed, for the first time, this loading information to be collected during extended off-road testing. In all, seven experienced riders rode a downhill trail test section with the test bicycle in both front-suspension and full-suspension configurations. The load histories were used quantitatively to describe the load components through the computation of means, standard deviations, amplitude probability density functions, and power spectral density functions. For the standing position, the coefficients of variation for the load components normal to the ground were greater than 1.2 for handlebar forces and 0.3 and 0.5–0.6 for the pedal and hub forces, respectively. Thus, the relative contribution of the dynamic loading was much greater than the static loading at the handlebars but less so at the pedals and hubs. As indicated by the rainflow count, high amplitude loading was developed approaching 3 and 5 times the weight of the test subjects at the front and rear wheels, respectively. The power spectral densities showed that energy was concentrated in the band 0–50 Hz. Through stress computations and knowledge of material properties, the data can be used analytically to predict the fatigue life of important structural components such as those for steering. The data can also be used to develop a fatigue testing protocol for verifying analytical predictions of fatigue life.

Introduction

Designers of off-road bicycles face a continual challenge to balance requirements for both light weight and adequate structural reliability. To be reliable, the design of either a bicycle frame or component must ensure adequate protection against failure under normal service loading conditions. Failure can occur either catastrophically from a single or limited number of extreme loads, or from fatigue arising from an accumulation of loads, which develop nominal stresses below the yield strength. In either case, the analytical procedures used to design a component must be founded on a knowledge of the loads the component experiences. While knowledge of both extreme and lower level fatigue loads is important, this research focused on quantifying the loads responsible for high cycle fatigue.

The loads applied to the bicycle can be characterized based upon their source of origin: rider induced, surface induced, or control induced. Rider-induced loads originate from active motions of the rider (i.e., pedaling actions) and from the rider's static weight. Surface-induced loads are the result of bicycle and rider inertial reactions caused by terrain irregularities. Finally, control-induced loads emanate from control inputs (e.g., steering and braking) by the rider. Of these three load categories, arguably the most important to fatigue failure in off-road bicycles is the surface induced because of the rough terrain over which off-road bicycles are typically used.

Despite the importance of surface-induced loading information to the design of reliable off-road bicycle components, relatively few studies have been directed toward providing this information. Using a dynamic system model and simulation, Wong and Hull (1983) computed surface-induced loads in an on-road environment characterized by generally smooth, prepared roads, which are not representative of off-road terrain. Subsequently, Wilczynski and Hull (1994) developed a dynamic system model for computing surface-induced loads during off-road cycling and made load measurements to verify the model. However, the measurements were made while coasting over an artificial surface, which was not representative of off-road surfaces encountered in practice. Considering the lack of information on surface-induced loads and the importance of this information to the design of off-road bicycles to resist fatigue failures, the research goal was to quantify these loads.

Methods

(A) Experiments. Surface-induced loading data were recorded from seven experienced recreational riders (some with cross-country and downhill racing experience). As rider weight has been shown to affect the magnitudes of some loads experienced by the bicycle during off-road riding (Stone and Hull, 1995), riders of approximately the same size were selected; the average height was 180 cm (standard deviation 4 cm) and the average mass was 75 kg (standard deviation 4 kg). To accommodate the test subjects, the only adjustment to the experimental bicycle was seat height.

The trail used for all experiments was fairly straight and continuously downhill of approximately 8 percent slope whose surface was rutted, washed-out, and held exposed rocks. This trail provided continuous surface excitation. Riders were instructed to travel as rapidly as possible while still maintaining adequate control. This instruction in conjunction with the trail surface required constant concentration from the riders, and allowed speeds in the range of 6–9 m/s (15–20 mph). Trials were done with the riders in

Contributed by the Bioengineering Division for publication in the JOURNAL OF BIOMECHANICAL ENGINEERING. Manuscript received by the Bioengineering Division February 12, 1998; revised manuscript received February 22, 1999. Associate Technical Editor: A. G. Erdman.

a standing position, crankarms nominally horizontal with the left foot forward, and using the front brake for speed control.

Riders took one practice run on a noninstrumented bicycle to familiarize themselves with the course, then rode down the hill twice on the experimental bicycle. The experimental bicycle was a state-of-the-art, full-suspension mountain bike (1995 FSR, Specialized Bicycle Components, Inc., Morgan Hill, CA) with a telescoping fork front-suspension and linkage-type rear-suspension. The two trials included one with full suspension and the other with front suspension (rear suspension motion disabled) and the order for each rider was chosen in a pseudo-random fashion. Front and rear suspension preload and air pressure were adjusted such that approximately one-third of the available travel was consumed by the rider's static weight. The cartridge-type damper used in the front fork was set to its lightest position; the rear shock damper remained in its factory configuration.

A reference frame was utilized to resolve the forces and moments measured on the bicycle. The frame was considered fixed to the bicycle, with the positive x direction pointing forward, the positive y direction normal to the plane of the frame and directed left, and the positive z direction making right angles with each of the previous axes and oriented upwards (Fig. 1).

Pedal forces were measured with a two-load component dynamometric pedal (Rowe et al., 1998). Loads were measured normal and tangential to the pedal surface on the right pedal. In order to resolve forces at the pedal into the bicycle reference frame, angular measurements of pedal-to-crank and crank-to-bike orientations were made. In the absence of pedaling, there was no tension in the bicycle drive chain. Since the sum of the torque about the bottom bracket must be zero, measurement of the forces in one pedal was sufficient to estimate the forces in the other pedal. First, the component of the pedal load perpendicular to the crank arm was sufficient to balance the corresponding load in the other pedal. Second, since the components of the pedal loads in the direction of the bicycle motion, or along the x axis, act to accelerate or decelerate the rider, both pedals were considered to have the same magnitude of force in this direction.

Forces at the front and rear ground contact patches were measured with dynamometric hubs (De Lorenzo and Hull, 1999), sensitive to x and z forces in the plane of the bicycle. Because braking loads at the rim will induce a reaction force at the hub that must be accounted for, strain gages were applied to the front brake to measure the retarding force acting on the front wheel due to front brake application. Front tire ground reaction forces were calculated from both the braking force and hub forces (Fig. 2). Although strain gages were also applied to the rear brake, the subjects were instructed not to use this brake. The strain gage output was recorded and checked to insure that the subjects followed the instruction. In the absence either of pedaling or rear braking, forces measured at the rear hub directly indicated the rear ground contact reaction forces.

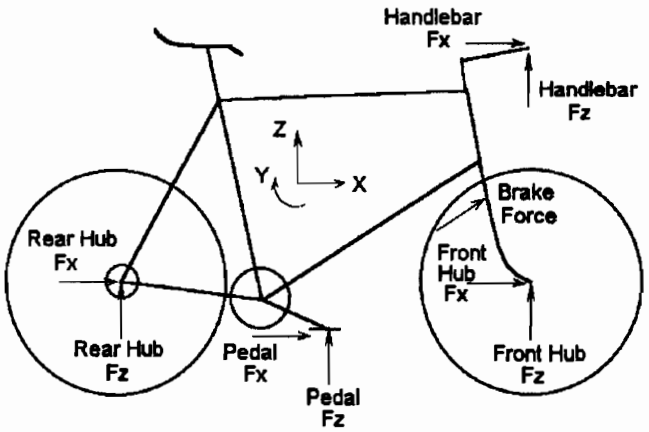

Fig. 1 Coordinate system and load components measured

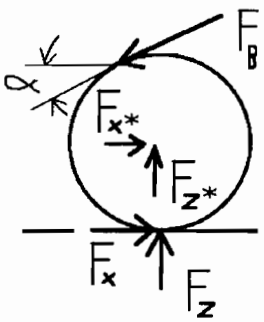

$$F_x = F_{xB} + F_{xG}$$

$$F_{xB} = -F_B$$

$$F_x = F_B \cos\alpha - F_{x^*}$$

$$F_{xG} = F_B (1+\cos\alpha) - F_{x^*}$$

$$F_z = F_B \sin\alpha - F_{z^*}$$

Fig. 2 Front wheel free-body diagram and equations for computing the ground contact forces due to the surface input separate from the braking input. F_{xB} and F_{xG} are the contributions to the tangential wheel force F_x from the brake and surface, respectively.

Hand reactions were measured with an instrumented handlebar sensitive to x and z axis forces on both the left and right sides of the handlebar. In this manner, the handlebar measured the total force acting from the rider's hands in the plane of the bicycle as well as the differential between the two hand contributions. This allowed the net torque about the steering axis (steering torque) and about the stem-extension axis to be calculated.

An additional transducer measured the speed of the bicycle. The bicycle linear velocity relative to the ground was determined from the rotational velocity of the rear wheel. A signal once per wheel revolution (nominally every $\frac{1}{4}$ s) was developed using an infrared emitter and detector mounted to the left seat-stay, with a beam-interrupting tab attached to the rear wheel spokes.

Data were logged in a purpose-built, portable data acquisition system allowing up to 32 channels of A/D input with 12-bit converter resolution, and equipped with 256K words of memory (Newmiller and Hull, 1990). For this application 21 analog/digital data acquisition channels were needed. Voltage signals from instrumentation were passed through conditioning circuitry to amplify and filter the input. A second-order Butterworth filter was set with a cut-off frequency of 50 Hz, which was above the maximum frequency of interest in order to minimize aliasing errors (Brigham, 1988). After each trial, the data stored in the portable computer were downloaded to a laptop computer.

Based on initial tests at higher sampling frequencies, which showed that the maximum frequency of interest was less than 50 Hz, the data were sampled at 4–5 times this value, which led to a 200 Hz sampling frequency. The total time of sampling for each rider was 60 seconds, which consisted of two 30 second trials.

(B) Analysis. The first step of the data analysis was to determine the equivalent loads using the pre-established voltage-to-load calibration data. The speed data then were processed from voltage spikes corresponding to each revolution of the rear wheel to determine the linear velocity of the bicycle. To compare the consistency of speeds among riders over the data collection interval, bicycle velocity for each rider, as well as average velocity of all riders, was plotted versus distance traveled.

To assess the validity and consistency of the collected data, a series of calculations was performed on the load histories. The averages of the total normal contact (z axis) forces measured both at the front and rear wheels and at the rider contact points were compared to the riders' weight. For wheel forces, this was done by summing the mean z component forces for each rider, normalizing by the weight of rider and equipment, and averaging over the 14 trials (7 subjects × 2 trials). In the case of rider contact forces, the mean z component force from each side of the handlebar was added to two times the right pedal z force (to account for both left and right pedal normal forces), normalized by the weight of rider and equipment, and averaged over the 14 trials. Also the averages

of the total tangential forces (i.e., x components) at the front and rear wheels and at the rider contact points were computed in a manner analogous to the z component calculations, and compared to the component of the riders' weight acting down the slope (i.e., (rider + equipment weight) × sin(tan^{-1} (0.08))). Note that this computation assumes that acceleration in the x direction is negligible. Inasmuch as the acceleration in this direction was less than 0.07 m/s^2 on average, the corresponding force required to accelerate an 850 N load is less than 6 N, which was considered negligible error. Finally, the mean values across trials of the net torques about the steering axis and the stem extension axis were computed.

Because the loads induced by the surface were of interest, the tangential ground contact force F_x at the front wheel was processed further. Note that the total tangential force component F_x depicted in Fig. 2 is the superposition of the ground contact force developed as a consequence of braking F_{xB} and the force developed as a consequence of rolling over the ground surface F_{xG}. Thus the tangential force was decomposed into the two contributions and F_{xG} was computed from the measured brake and hub dynamometer loads using the equations given in Fig. 2. F_{xG} was used in the analyses to quantify the loading.

Because of their relation to the procedures used for fatigue failure analysis, correlation coefficients were computed for various pairs of force components. To compute these coefficients, the data from both trials of all riders were used.

To describe the loads quantitatively, the basic statistics (i.e., mean and standard deviation) were computed for each of the two bicycle setups (i.e., rear suspension active and inactive) and for each rider. For each setup, these statistics were then averaged over the seven riders. The coefficient of variation for each load component and bicycle setup was then computed to assess the relative contribution of the dynamic loading to the static loading. Also, a paired t-test was done on standard deviations to determine whether the bicycle setup influenced the dynamic loading.

In addition to the basic statistics, a second analysis computed the amplitude probability density functions for each load component. Because of the usefulness to fatigue life prediction of quantifying the number and magnitude of load reversals, these functions were computed via a rainflow counting algorithm. As with the basic statistics, these functions were computed for each bicycle setup and rider and then averaged over all seven riders for each setup. To compute the amplitude probability density functions, the loading was divided into 20 N increments, intermediate load values were first removed from the loading history so that all that remained were relative peaks and valleys. Then the load ranges in the loading history, from the lowest negative value to the highest positive value and all intermediate ranges in between, were tabulated.

Power spectral densities of the load histories were computed via a fast Fourier transform (FFT) algorithm (Brigham, 1988) primarily to establish that the selected sampling rate of 200 Hz offered sufficient bandwidth. After the mean value was subtracted, a Hanning window was applied to the time series records to reduce leakage effects at the start and end of each record. The resulting spectra were computed and averaged over all riders to reduce the magnitude of the random error (Bendat and Piersol, 1986). To keep the normalized random error in power spectral density calculations below 25 percent, a total of $1/(0.25)^2 = 16$ records was averaged for each subject; after results were averaged over all seven riders, the normalized random error in power spectral density estimates was reduced below 10 percent. With a record length of 3.75 seconds, this yielded a resolution bandwidth of (1/3.75 s) or 0.26 Hz.

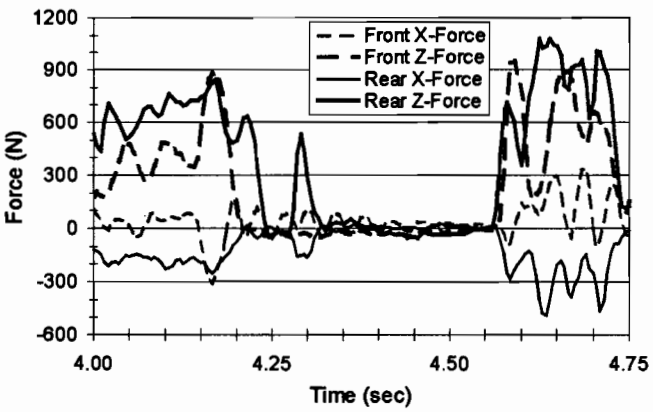

Fig. 3 Sample segment of wheel force components time series

Table 1 Correlation coefficients for various force component pairs

Force Components	Correlation Coefficient
Handlebar Left Side Fx and Fz	-0.82
Handlebar Right Side Fx and Fz	-0.79
Handlebar Left Side Fx and Right Side Fx	0.93
Handlebar Left Side Fz and Right Side Fz	0.82
Steering and Stem-Extension Torques	0.12
Steering Torque and In-Plane Bending	0.06
Stem-Extension Torque and In-Plane Bending	-0.04
Steering Torque and Front Wheel Fx	0.10
Steering Torque and Front Wheel Fz	-0.01
Pedal Fx and Pedal Fz (w.r.t. bike frame)	-0.02
Front Wheel Fx and Fz	-0.38
Rear Wheel Fx and Fz	-0.81

Results

The mean total normal contact force measured at the front and rear wheels equaled the total weight of the rider and equipment (ratio between mean normal forces and total weight equal to 0.95 ± 0.04), and the mean total tangential wheel force was equal to that amount required to keep the bicycle and rider at constant velocity down an 8 percent incline (average measured force −61 ± 41 N). The mean z axis (nominally vertical) forces measured at the rider contact points were equal to the total weights of the riders and equipment (ratio between mean normal forces and total weight equal to 0.96 ± 0.02). The mean total tangential force measured at the left and right sides of the handlebar and at the right pedal (and multiplied by 2), while not in close agreement, did overlap the range predicted from tangential force measurements taken at the hubs (average measured force −12 ± 54 N); the variability in the data is attributable to the limitation of using one pedal to estimate the net tangential force caused by the rider's feet. At the handlebar, the net torque values were found to be indistinguishable from zero (average steering axis torque equal to −0.12 ± 2.5 Nm and average stem-extension torque equal to −0.23 ± 0.64 Nm, as would be expected in order to ride in a nominally straight line with rider weight centered laterally over the bike.

As examples of load histories, time series were reproduced from representative hub, pedal, and handlebar force measurements (Figs. 3–6). The hub force data (Fig. 3) were taken from a section of trail near the beginning of each data collection run, which contained a rock off of which riders were instructed to jump. From these data, the takeoff and landing techniques of this rider are apparent. At the beginning of the jump, the front wheel left the ground first, after being preloaded by the rider. As the rear wheel passed over the same terrain, it left the ground as well. In the air, the forces on the wheels went to zero, as the bike traveled in a parabolic trajectory. Since the vertical forces on both wheels increased simultaneously on landing, it is evident that the rider landed flat, with both wheels contacting the ground at the same instant of time. This rider traveled approximately 2.5 m airborne.

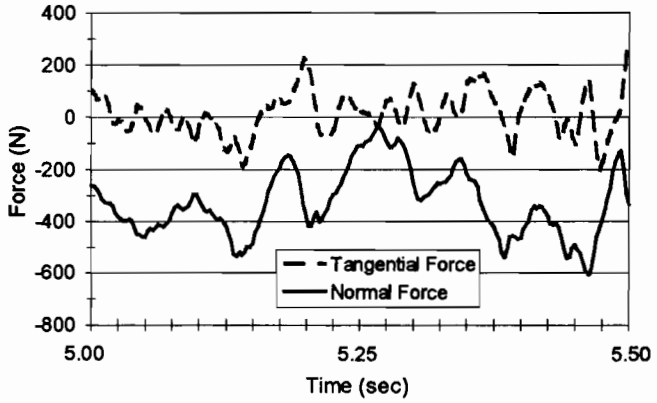

Fig. 4 Sample segment of pedal force components time series

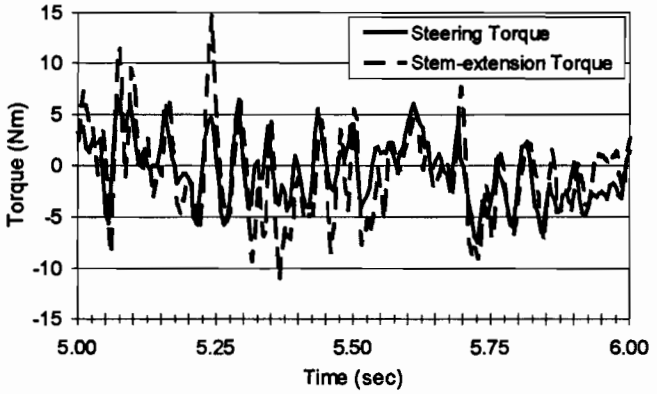

Fig. 6 Sample segment of steering and stem-extension torques time series

Finally, notice that the correlation between the two components on a particular hub, and hence the two ground contact force components for a particular wheel, is weak. For the front wheel, which is of primary interest, the correlation coefficient was −0.38 (Table 1). The negative sign occurred because the impact loads at the front wheel impart a negative x force and a positive z force.

Pedal data (Fig. 4) show that this rider supported approximately 300 N of his weight on the right pedal (which contained the dynamometer); therefore, 75 percent of the weight of this rider (total weight 800 N) was supported by his feet. The average weight supported in the tangential direction was near zero, as would be expected with the rider traveling at a nominally constant velocity. With a correlation coefficient of only 0.02 (Table 1), the two load components were completely unrelated.

As expected, the handlebar data (Fig. 5) illustrate high correlations between x and z axis force components measured on the same side of the handlebar (correlation coefficients of −0.82 and −0.79 for left and right, respectively) as well as between the same force components measured on opposite sides of the handlebars (correlation coefficients of 0.81 and 0.93 for x and z axis forces, respectively) (Table 1). Although the data indicated relatively small instantaneous differences in respective right and left force components, the torques about the steering and stem extension axes were substantial (Fig. 6). Peak steering torques exceeded 5 Nm while peak extension torques about the stem extension axis were greater, reaching 15 Nm. The relatively large torques developed because of the leverage of the forces acting through the handlebars, which offered a moment arm of about 0.3 m. Steering and stem-extension torques were not correlated to each other (coefficient = 0.12) (Table 1) since rider control actions (steering torques) were not related to the impact loads reacted by the rider's hands, which cause a moment about the stem-extension axis. Also neither load component was correlated to the bending moment developed on the stem extension in the plane of the bicycle (coefficients = 0.04 and 0.06).

Speeds among the riders were similar during data collection (Fig. 7). The average speeds while riding with full suspension (8.8 ± 0.9 m/s) versus riding with front suspension only (8.7 ± 1.0 m/s) were the same with the riders covering an average of 260 ± 30 m in a 30 second trial. Speeds were uniformly lower, and reflected more braking, at the beginning of the trials where the ground was rockier, and increased toward the end of the run, where the trail became smoother and wider. In fact, in the section of trail corresponding to about 180 m to 240 m, riders were able to let off the front brake entirely and coast in a sort of free-fall (average acceleration equal to 0.244 m/s^2 or 0.025 g); this is borne out by the front brake force data as well.

Loads measured at the front and rear wheels and pedals had large mean values in the z direction (i.e., normal to the riding surface) (Table 2), which was expected because the majority of the rider's weight was supported in that direction. At these points the dynamic contribution to the loading in the z direction was relatively low compared to the static contribution, as evidenced by the small coefficients of variation, which ranged from about 0.3 at the pedal to 0.6 at the front wheel. In contrast to these was the coefficient of variation for the handlebars for the z-directed force component; because the riders evidently supported little weight on the handlebars, the coefficient of variation was greatest at this contact point in the z direction, exceeding 1.2. Because the mean values for all x-directed force components were small, the dynamic contribution to the loading was substantial, as evidenced by the higher coefficients of variation. Despite disparities in the coefficients of variation in the x and z directions, the dynamic loading

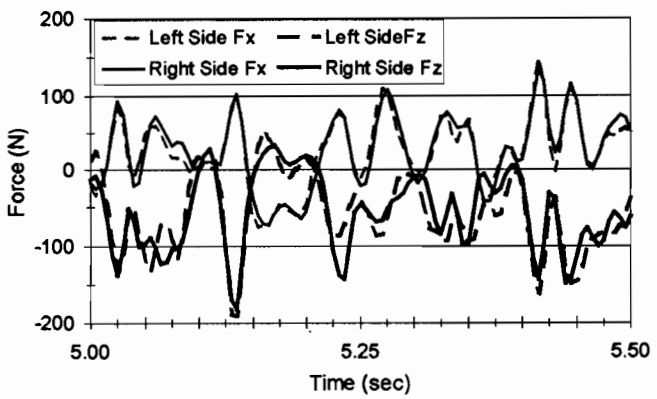

Fig. 5 Sample segment of handlebar force components time series

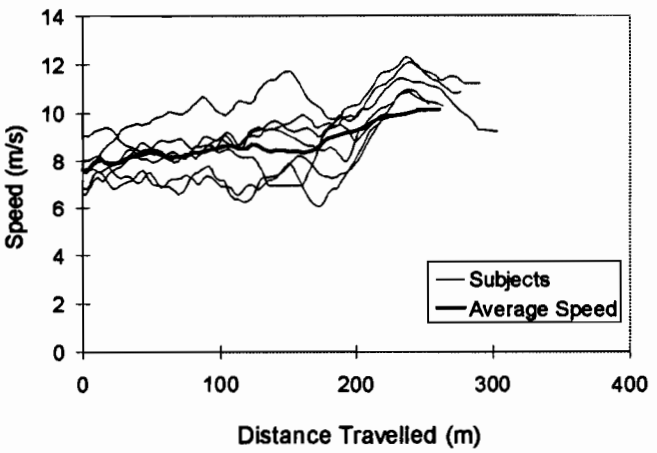

Fig. 7 Forward velocity during front suspension trials

Table 2 Mean load values, standard deviations, and coefficients of variation. Also, *t*-test results are included that indicate the effect of the suspension configuration.

		Full Suspension	Front Suspension	T-Test p Values
Handlebar Left Side Fx	Mean (N)	-4.56	1.97	0.0002
	St. Dev (N)	48.43	54.74	
	Coef.of Var.	10.62	27.79	
Handlebar Left Side Fz	Mean (N)	-28.39	-36.24	0.041
	St. Dev (N)	41.92	43.75	
	Coef.of Var.	1.48	1.21	
Handlebar Right Side Fx	Mean (N)	-4.78	0.10	0.001
	St. Dev (N)	50.20	54.66	
	Coef.of Var.	10.50	546.60	
Handlebar Right Side Fz	Mean (N)	-31.89	-33.10	0.389
	St. Dev (N)	44.35	43.94	
	Coef.of Var.	1.39	1.33	
Front Wheel Fx	Mean (N)	19.40	-4.32	0.146
	St. Dev (N)	96.52	102.71	
	Coef of Var.	4.96	23.78	
Front Wheel Fz	Mean (N)	219.32	222.80	0.440
	St. Dev (N)	132.26	132.82	
	Coef.of Var.	0.60	0.60	
Rear Wheel Fx	Mean (N)	-30.74	-22.34	0.002
	St. Dev (N)	100.45	114.01	
	Coef.of Var.	3.27	5.10	
Rear Wheel Fz	Mean (N)	536.15	517.29	0.000
	St. Dev (N)	265.87	311.18	
	Coef.of Var.	0.50	0.60	
Pedal Fx (w.r.t. frame)	Mean (N)	-9.75	1.60	0.001
	St. Dev (N)	51.76	62.74	
	Coef.of Var.	5.31	39.21	
Pedal Fz (w.r.t. frame)	Mean (N)	-345.54	-341.18	0.077
	St. Dev (N)	101.68	112.06	
	Coef.of Var.	0.29	0.33	
Front Brake	Mean (N)	40.84	42.76	0.437
	St. Dev (N)	45.70	45.15	
	Coef.of Var.	1.12	1.06	
Steering Torque	Mean (N)	0.20	-0.61	0.468
	St. Dev (N)	4.91	4.90	
	Coef.of Var.	24.55	8.03	
Stem-extension Torque	Mean (N)	0.71	-0.78	0.414
	St. Dev (N)	6.00	6.06	
	Coef.of Var.	8.45	7.77	

was surprisingly consistent in the x and z directions at the front wheel and handlebars, where the standard deviations for respective x and z components were comparable.

The results of the paired t-tests indicated that the use of the rear suspension led to significant reductions in the dynamic loading at the rear tire, which was expected. Significant reductions in dynamic loads were also evident in other load components as well, which was unexpected. Specifically, all load components in the x direction were significantly reduced except at the front wheel.

The amplitude probability density functions demonstrated that high load ranges were developed at all contact points. From the sample results illustrated (Fig. 8), the rainfall count registered higher load ranges in the x-directed than the z-directed force components. Although difficult to appreciate from Fig. 8 because of the scale on the vertical axis, load ranges above 500 N occurred 13 times in the x direction and only one time in the z direction at the handlebar. At the front wheel, the loading exceeded 1500 N three times in the x direction while no ranges above this level were recorded in the z direction.

For all load components the majority of off-road excitation occurred below 50 Hz (Fig. 9), justifying the use of a 200 Hz sampling frequency required to minimize aliasing errors.

Discussion

The objective of the work reported in this article was to quantify the loading during actual off-road cycling for input into methods

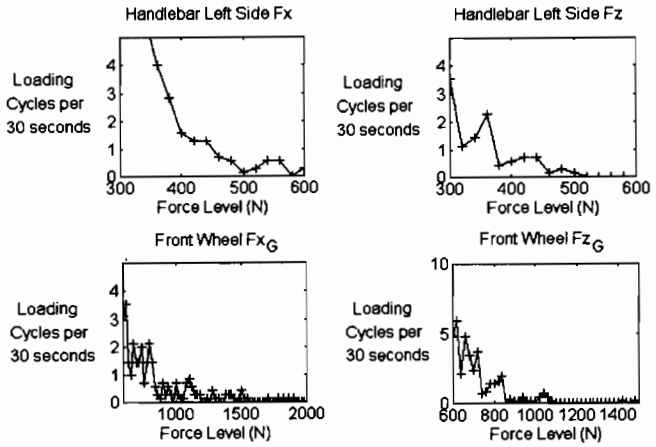

Fig. 8 Rainflow counting results averaged over the seven subjects for handlebar left side and front wheel time histories under front suspension configuration

for fatigue life prediction and testing. Because the loads encountered by an off-road bicycle are dependent upon many variables, which fall into three categories that include the properties of the rider, the terrain, and inherent qualities of the bicycle itself, consideration was given to limiting the scope of the study. The scope was limited by having riders of relatively consistent weight coast over one type of terrain in a standing posture while riding the same test bicycle. As a consequence of having the riders coast, only the surface-induced loads were measured. Since the loads resulting from surface irregularities are most likely to undergo large reversals, thus giving rise to fatigue damage, and loads contributed by rider pedaling actions are well known, the surface-induced loads were of primary interest. To generate loading that includes both surface and rider induced, the two types of load could be superimposed from separate measurements.

With the riders in the standing position, the rider contact points included the pedals and the handlebars but excluded the seat. Inasmuch as the components most susceptible to fatigue failure in practice are the forks, handlebars/stem, and frame at the head tube-down tube junction, the measurements provided loading information relevant to the components of greatest interest.

As described previously, the downhill-sloped trail surface could be described as rutted, washed-out, and exposing rocks. This trail provided continuous surface excitation with high-magnitude inertial loads. The maximum magnitude forces measured during ex-

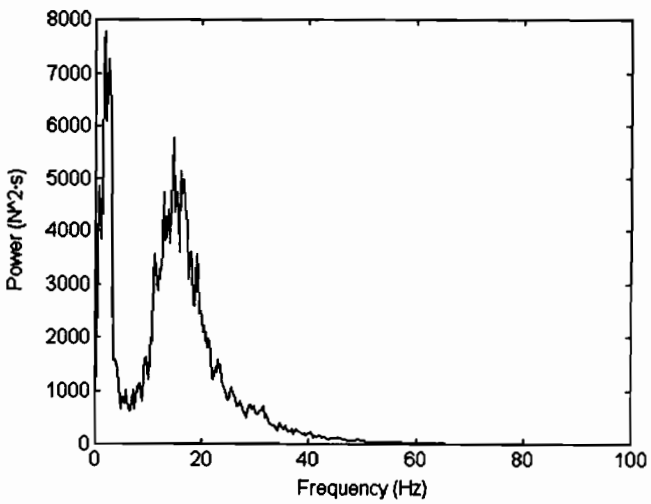

Fig. 9 Power spectral density for rear wheel *z*-force time histories under front suspension configuration

perimental trials were 1900 N for the front wheel contact and 4000 N for the rear wheel contact, which was about three and five times the weight of the riders, respectively. These loads were consistent with those measured in preliminary tests, which were conducted to determine static strength requirements of the hub dynamometers. Using a force plate to measure the forces generated at the front and rear wheels during impact with the ground indicated that impact loads of at least five times rider weight could be encountered on each wheel. Accordingly the combination of trail surface and speed elicited loads that would be useful for meaningful calculations of fatigue life during aggressive off-road cycling.

To compute statistical measures of the loads that reflected different riding styles independent of weight, the riders were all of similar weight and height. As a consequence, calculations of fatigue life are meaningful only for the subject sample tested. Presumably changes in rider weight would be reflected in direct scaling of both mean and dynamic loads at least over some range of weights. This presumption is based on the notion that the dynamic loads are inertial and hence would scale directly according to the rider's mass. If this assumption were valid, then the loads reported herein could be scaled to develop a data set for making fatigue life estimates for riders of arbitrary weight. Thus, it would be useful to check this assumption experimentally in a future study and use the results from such a study to develop the scaling laws if appropriate.

The results may be applicable to only a single bicycle for the suspension settings used in the tests. As the statistical comparison between the two suspension configurations demonstrated, the dynamic contribution to the loading was different depending on the configuration. Given this dependence, it could also be expected that the loading would be affected by the settings for stiffness and damping on a particular suspension component.

Also the unexpected result that the dynamic loads were reduced significantly for the x-directed rear wheel load component for the full suspension configuration suggests that the results may be applicable to only a single design as well. The test bicycle achieved the rear suspension function using a four-bar linkage. Depending on the linkage design, it is possible to develop a motion path of the rear axle that is x-directed to some degree. For such a design the suspension could act to absorb dynamic rear wheel loads in both the x and z directions, thus attenuating both load components over the front suspension only configuration. However, other suspension designs (e.g., single swing arm) that do not offer any substantial amount of x-directed rear axle travel may not significantly attenuate the x-directed component of the wheel force.

To determine whether the load data recorded for a particular mechanism with specific settings would serve as a universal data set for fatigue life predictions and verification tests, it would be necessary to compare statistically the rainflow counts computed from loading data recorded for various mechanisms used at various settings. Considering the wide variety of mechanisms that is commercially available and the variability in suspension settings offered by individual mechanisms, this would be a formidable task.

In considering the components of greatest interest from a fatigue failure standpoint, these would include the components involved in steering (i.e., handlebars, stem, and fork) (Hull, 1996) because structural failure of any of these would cause a potentially serious accident. The results from the load quantification provide some guidance toward the procedures that would need to be followed in fatigue life prediction and testing. In the case of the handlebars, although the correlation between the x and z force components was strong (Table 1), the R-squared value indicated that about 35 percent of the variability was not explained by the linear model. Thus the direction of worst-case loading would need to be determined. To make this determination, the time series would need to be computed for different orientations around the cross section. Then a procedure such as the rainflow method would need to be used to count the number of the stress (or strain) reversals for each orientation time series. Finally a cumulative damage criterion such as Miner's rule would need to be applied to determine the loading direction of maximum damage. Once this direction was identified, then this would be used for fatigue life estimation and testing because it would correspond to the direction of minimum life. Because the handlebar loads create uniaxial stresses, the application of loads to conduct a meaningful fatigue test is simplified.

The stem is more complicated than the handlebars because there are two different regions of failure and because the loading is multi-axial and not proportional in either region. The two different regions are the extension, which contains the handlebar clamp, and the quill, which inserts into the steerer tube of the fork. The extension experiences multiplane bending because it is loaded not only in the plane of the bicycle but also because it is loaded by the steering torque. Because the steering torque is not strongly correlated to the in-plane bending, the plane of maximum damage is not obvious and would need to be determined using a procedure similar to that for the handlebars described above. However, the effects of the stem extension torque must still be considered. Since this torque is uncorrelated to the in-plane bending (Table 1), a multi-axial loading situation is developed where the stresses/strains are nonproportional. Accordingly a multi-axial fatigue life estimation theory would need to be used. Among the possible theories are equivalent stress-life and equivalent strain-life approaches, Sines Method, and critical plane approaches. The multi-axial nature of the loading complicates not only the life prediction, but also the testing. These same observations also apply to the quill because the stem extension torque causes multi-plane bending and the steerer torque causes multi-axial loading.

In the absence of braking, the fork is loaded by both the wheel forces and the steering torque. As with the wheel forces, the steering torque causes bending of the fork blades predominantly in the plane of the bicycle, but the direction of bending in the two blades is opposite. This predominance arises because the steering axis is about 17 deg with respect to vertical. However, because the steering torque is uncorrelated to the front wheel forces (Table 1), the two types of loads may be considered separately. Similar to the handlebars and stem, the loading direction of maximum damage due to the wheel forces needs to be determined. This need is readily apparent from the weak correlation of only -0.38 between the x and z wheel force components (Table 1). Accordingly the procedures described above to find the loading direction of maximum damage would need to be applied except that the component of the vector perpendicular to the steering axis would be computed for each of the time series because the stresses due to bending would dominate over those due to axial loading. Once the time series causing maximum damage from the wheel forces was determined, the time series of the reaction loads at the hub due to the steering torque would then be superimposed and the rainflow count would be performed on the stresses developed as a result of the superimposed time series of the forces. Thus, in the absence of braking, the fatigue life of the fork may be predicted using methods appropriate for uniaxial loading. In the presence of braking, the life prediction of the fork becomes more complicated, because the brake reaction loads create torsion on the fork blades, which gives rise to a multi-axial stress state.

Conclusions

The contributions of this study are as follows:

1 An instrumentation system to measure loading inputs to the bicycle structure at all points of input has been described. With the information provided by this system, loads in any structural component of interest can be determined.

2 Loads during actual off-road cycling have been measured and analyzed. These data now allow engineering analysis techniques to be applied in the optimal design of bicycle structural components. As evidenced by the many structural failures in practice (Morgan, 1998), there is a need for these data to be used in this context. In addition, these data will allow for the meaningful

development of testing methods by standards organizations such as the American Society for Testing and Materials (ASTM) to verify designs (Hull, 1996).

3 The bandwidth of the loading at the contact points has been determined and is bounded by about 50 Hz. This bandwidth establishes that the appropriate sampling frequency to avoid aliasing and at the same time to minimize memory requirements in data acquisition is 200 Hz.

4 In analyzing and comparing the dynamic loads for the front-only suspension versus the full suspension, the advantage of the full suspension in reducing the dynamic loads has been demonstrated. This result implies that the suspension design influences the life of structural components.

5 A correlation analysis of various force component pairs has been performed and the results have been used to identify methods of fatigue life prediction and testing applicable to steering components. Three results of significance to practical bicycle design that have not been recognized previously are as follows: (*i*) the need to analyze handlebar failure according to the direction of maximum damage, (*ii*) the need to apply methods of multi-axial fatigue failure analysis to both the extension and quill portions of the stem, and (*iii*) the need to analyze the fork blades according to the direction of maximum damage.

Acknowledgments

The authors express their gratitude to the following companies for their financial support: Cannondale, Dunlop Cycles, Easton, GT Bicycles, Mavic, Rockshox, Specialized Bicycle Components, Trek Bicycle Corporation, and True Temper Sports.

References

Bendat, J. S., and Piersol, A. G., 1986, *Random Data—Analysis and Measurement Procedures,* Wiley, New York, Chaps. 8 and 11.

Brigham, E. O., 1988, *The Fast Fourier Transform and Its Applications,* Prentice-Hall, Englewood Cliffs, NJ, Chaps. 6–9.

De Lorenzo, D. S., and Hull, M. L., 1999, "A Hub Dynamometer for Measurement of Wheel Forces in Off-Road Bicycling," ASME JOURNAL OF BIOMECHANICAL ENGINEERING, Vol. 121, pp. 137–142.

Hull, M. L., 1996, "Progress Towards Voluntary Standards for Bicycles in the United States," *Cycling Science,* Vol. 8(2), pp. 11–13.

Morgan, J. E., 1998, "The Recurrent Failure of Modern Bicycle Components," in: *The Engineering of Sport,* S. J. Haake, ed., Blackwell Science, Malden, MA, pp. 153–162.

Newmiller, J., and Hull, M. L., 1990, "A 6800 Based Portable Data Acquisition Module With Advanced Performance Capabilities," *International Journal of Sports Biomechanics,* Vol. 6, pp. 404–414.

Rowe, T., Hull, M. L., and Wang, E. L., 1998, "A Pedal Dynamometer for Off-Road Bicycling," ASME JOURNAL OF BIOMECHANICAL ENGINEERING, Vol. 120, p. 161.

Stone, C., and Hull, M. L., 1993, "Rider/Bicycle Interaction Loads During Standing Treadmill Cycling," *Journal of Applied Biomechanics,* Vol. 9, pp. 202–218.

Stone, C., and Hull, M. L., 1995, "The Effect of Rider Weight on Rider-Induced Loads During Common Cycling Situations," *Journal of Biomechanics,* Vol. 28, pp. 365–375.

Wilczynski, H., and Hull, M. L., 1994, "A Dynamic System Model for Estimating Surface Induced Frame Loads During Off-Road Cycling," ASME *Journal of Mechanical Design,* Vol. 116, pp. 816–822.

Wong, M. G., and Hull, M. L., 1983, "Analysis of Road Induced Loads in Bicycle Frames," ASME *Journal of Mechanisms, Transmissions and Automation in Design,* Vol. 105, pp. 138–145.